PHYSICAL REVIEW A **75**, 051801(R) (2007)

Preparation and determination of spin-polarized states in multi-Zeeman-sublevel atoms

Bo Wang,[1] Yanxu Han,[1] Jintao Xiao,[1] Xudong Yang,[1] Chunhong Zhang,[1] Hai Wang,[1,*] Min Xiao,[1,2] and Kunchi Peng[1]
[1]*The State Key Laboratory of Quantum Optics and Quantum Optics Devices, Institute of Opto-Electronics, Shanxi University, Taiyuan, 030006, People's Republic of China*
[2]*Department of Physics, University of Arkansas, Fayetteville, Arkansas 72701, USA*
(Received 16 November 2006; published 2 May 2007)

We demonstrate a simple, all-optical technique to prepare and determine the desired internal quantum states in multi-Zeeman-sublevel atoms. By choosing appropriate coupling and pumping laser beams, atoms can be easily prepared in a desired Zeeman sublevel with high purity or in any chosen ground-state population distributions (spin-polarized quantum-state engineering). The population distributions or state purities of such prepared atomic states can be determined by using a weak, circularly polarized probe beam due to differences in transition strengths among different Zeeman sublevels. This technique will have potential impact on quantum-information processing in multilevel atomic systems.

DOI: 10.1103/PhysRevA.75.051801 PACS number(s): 42.50.Gy, 03.65.Wj, 32.80.Pj

Preparing atoms into one specified internal quantum state and determining the population distribution in multi-Zeeman-sublevel atomic systems are very important in studying atom-field interactions, especially interesting schemes for quantum-information processing (QIP) such as light storage [1], quantum phase gate [2–5], and entanglement between atomic assemble and photons [6] or between a single trapped ion and a single photon [7]. Demonstrations of these effects require more than two atomic energy levels and a well-defined initial internal quantum state for the atoms, which cannot be accomplished by simple optical pumping as in the case for a two-level atomic system. Although in most cases interesting effects can be experimentally demonstrated by simply considering degenerate Zeeman levels, so no specific ground-state population preparations are needed [as in the cases of electromagnetically induced transparency (EIT) [8–10] and photon storage [11,12]], there are many effects that demand better quantum-state preparation and determination in the multi-Zeeman-sublevel atomic systems. For example, in order to demonstrate a quantum phase gate in multilevel atomic systems, such as the five-level M-type [3] and five-level combined M and tripod-type [5] systems, initial ground-state populations have to be prepared in specific Zeeman sublevels. Another example is the synthesis of arbitrary quantum states with atoms [13]. Several techniques were developed previously to prepare and determine the ground-state populations in multi-Zeeman-level atomic systems by using a magnetic field [14–17] or microwave field [18–20], or light-induced momentum transfer [21,22]. These experiments were all done in atomic beams or in atomic vapor cells, and they are too cumbersome to be used for QIP experiments, especially since they are strong measurements which erase the prepared original quantum state [23]. More importantly, most of these techniques cannot be used for cold atoms trapped by a magneto-optical trap (MOT), in which the magnetic field has to be near zero at the center and it could be difficult to apply a strong microwave field. Reference [23] demonstrated a method to estimate the prepared quantum state in cold atoms with weak measurement by probing the Lamor procession and Wigner function reconstruction, which is an indirect way with complicated data processing. Since many recent experiments on QIP were done in cold atoms in a MOT (such as [6,11,12]), it is necessary to develop a new technique that can prepare and directly determine the spin-polarized states in multi-Zeeman-level systems without employing a magnetic field or microwave field, and without destroying the prepared spin-polarization states in the measurements.

In this Rapid Communication, we present a simple procedure to prepare any desired internal quantum states at various Zeeman sublevels, and more importantly, we demonstrate an all-optical technique to determine the ground-state population distributions simply by applying a weak, circularly polarized probe laser beam. The preparation of a desired quantum state is achieved by combining optical pumping from two polarized laser beams. The basic mechanism for detecting and determining the prepared internal quantum state is to make use of the differences in transition strengths among different Zeeman sublevels (different Clebsch-Gordan coefficients), as shown in Fig. 1(b), and the changes in the corresponding multi-dark-state resonances (MDSR) [as shown in Fig. 1(c)] [24]. By combining the measured probe spectrum with the theoretical calculation, one can easily determine the ground-state population distribution and the purity of the prepared quantum state with high precision. This technique of determining the prepared spin-polarized states has several advantages over the previously demonstrated ones since it is all-optical with direct measurement and fast response, and it does not destroy the prepared spin-polarized states, which is ideal for QIP experiments using cold atoms in a MOT.

The experiment was performed with the D1 line of ^{87}Rb atoms, as shown in Fig. 1(b), in a vapor cell magneto-optical trap (MOT) which is the same as in Ref. [24]. A strong coupling beam with linear polarization in the z direction [as shown in Fig. 1(a)] propagates along the x axis through the cold atoms while a weak, left-circularly polarized probe beam propagates along the z axis through the atoms. The diameters of the coupling and probe beams are 2.6 and

*Corresponding author. Email address: wanghai@sxu.edu.cn

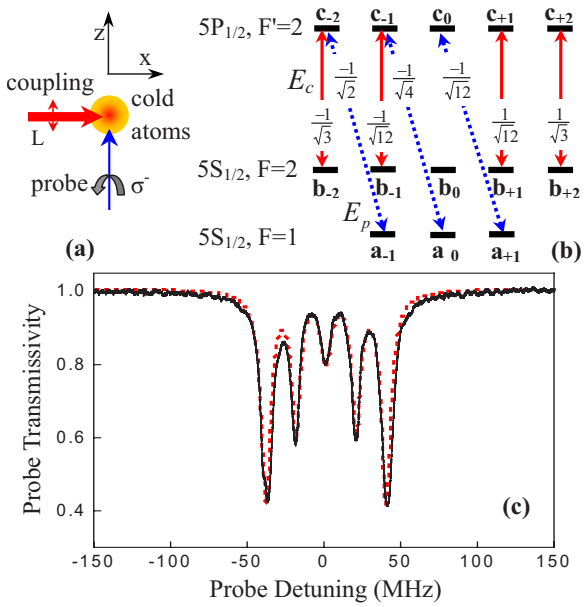

FIG. 1. (Color online) (a) Experimental setup. (b) Relevant atomic energy levels interacting with the probe (dotted lines) and coupling (solid lines) laser beams. (c) Transmission spectrum of the probe beam. The solid line is the experimental result and the dotted line is the theoretical fitting curve corresponding to $P_{a_{-1}}=32\%$, $P_{a_0}=36\%$, $P_{a_{+1}}=32\%$, and $N_{F1}=1.2\times10^{11}$ cm^{-3}. Other parameters are $\Omega_{c2}=78$ MHz, $\Omega_{p2}=1$ MHz, $l=2$ mm, $\gamma_{ab}=2$ MHz, and $\gamma_{ac}=4$ MHz (γ_{ab} and γ_{ac} include the laser linewidths).

0.5 mm, respectively. A uniform, weak magnetic field of about 150 mG in the z direction is applied at the location of the cold atoms. During the experiment, the on-off sequence of the trapping, repumping, coupling, and probe beams is controlled by four acousto-optical modulators. The coupling beam is switched on at the same time as the MOT is turned off, 0.1 ms later, the probe beam is turned on.

As shown in Fig. 1(b), a linearly polarized coupling beam E_c (frequency ω_c) drives transition $5S_{1/2}$, $F=2$ to $5P_{1/2}$, $F'=2$, and a left-circularly polarized probe beam E_p (frequency ω_p) scans through the transition $5S_{1/2}$, $F=1$ to $5P_{1/2}$, $F'=2$. The probe field Ω_{p2} (connecting states $|a_{-1}\rangle$ and $|c_{-2}\rangle$) and the coupling field Ω_{c2} (connecting states $|b_{-2}\rangle$ and $|c_{-2}\rangle$) form an EIT system, which has an EIT window much broader than the EIT window formed by the probe field Ω_{p1} (connecting states $|a_0\rangle$ and $|c_{-1}\rangle$) and the coupling field Ω_{c1} (connecting states $|b_{-1}\rangle$ and $|c_{-1}\rangle$) since $\Omega_{c2}=2\Omega_{c1}$ [24]. Since the transition strength between states $|b_0\rangle$ and $|c_0\rangle$ is zero, the probe field Ω_{p0} (connecting states $|a_{+1}\rangle$ and $|c_0\rangle$) has a simple absorption peak. Here, Ω_{p0}, Ω_{p1}, and Ω_{p2} are Rabi frequencies for the same probe laser beam E_p corresponding to different transitions and similarly, Ω_{c1} and Ω_{c2} are the Rabi frequencies for the same coupling field E_c corresponding to different transitions. When the probe beam scans through the transition from $5S_{1/2}$, $F=1$ to $5P_{1/2}$, $F'=2$, one observes the multiple EIT peaks (or MDSR), as shown in Fig. 1(c) [24].

The susceptibilities of the probe field coupling the states $|a_{-1}\rangle\rightarrow|c_{-2}\rangle$, $|a_0\rangle\rightarrow|c_{-1}\rangle$, and $|a_{+1}\rangle\rightarrow|c_0\rangle$ are

$$\chi_{a_{-1}c_{-2}}=-P_{a_{-1}}N_{F1}\rho_{a_{-1}c_{-2}}|\mu_{a_{-1}c_{-2}}|^2/(\hbar\varepsilon_0\Omega_{p2}),$$

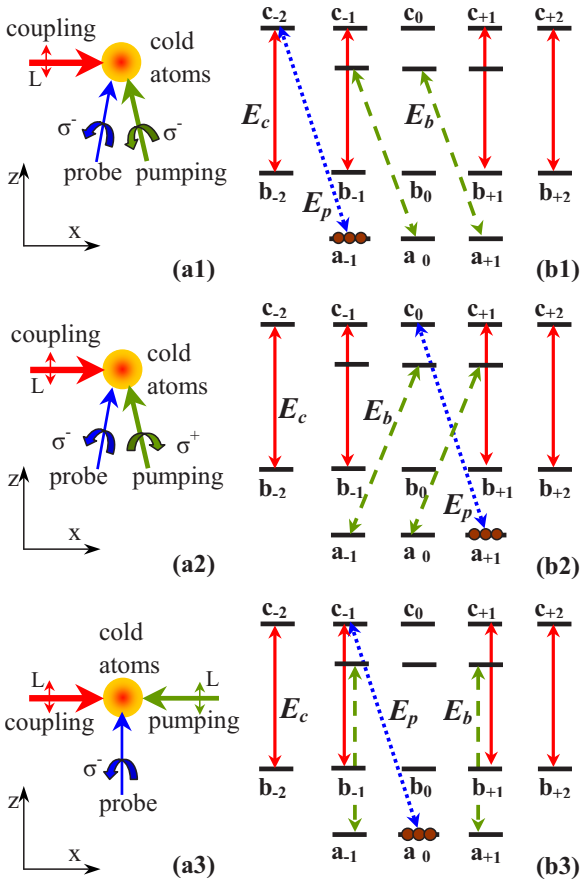

FIG. 2. (Color online) Different polarized pumping beam schemes. (a1)–(a3) Experimental setups for different laser beam propagation and polarization directions. (b1)–(b3) Relevant atomic energy levels with interacting laser beams. Solid (red) lines are coupling fields; dotted (blue) lines are probe fields, and dashed (green) lines are pumping fields.

$$\chi_{a_0c_{-1}}=-P_{a_0}N_{F1}\rho_{a_0c_{-1}}|\mu_{a_0c_{-1}}|^2/(\hbar\varepsilon_0\Omega_{p1}),$$

and

$$\chi_{a_{+1}c_0}=-P_{a_{+1}}N_{F1}\rho_{a_{+1}c_0}|\mu_{a_{+1}c_0}|^2/(\hbar\varepsilon_0\Omega_{p0}),$$

respectively, where $P_{a_{-1}}$, P_{a_0}, and $P_{a_{+1}}$ are the populations of the ground states $|a_{-1}\rangle$, $|a_0\rangle$, and $|a_{+1}\rangle$, respectively. N_{F1} is the total density of atoms staying in the energy levels of $5S_{1/2}$, $F=1$. $\mu_{a_{-1}c_{-2}}$, $\mu_{a_0c_{-1}}$, and $\mu_{a_{+1}c_0}$ are the dipole moments for $|a_{-1}\rangle\rightarrow|c_{-2}\rangle$, $|a_0\rangle\rightarrow|c_{-1}\rangle$, and $|a_{+1}\rangle\rightarrow|c_0\rangle$ transitions, respectively. The density-matrix elements $\rho_{a_{-1}c_{-2}}$, $\rho_{a_0c_{-1}}$, and $\rho_{a_{+1}c_0}$ can be calculated by solving the density-matrix equations involving all Zeeman sublevels in the system [25]. The total probe field susceptibility is given by $\chi=\chi_{a_{-1},c_{-2}}+\chi_{a_0,c_{-1}}+\chi_{a_{+1},c_0}$. The probe transmissivity T is given by

$$T=\exp[-\omega_p\mathrm{Im}(\chi)l/c], \quad (1)$$

where l is the diameter of cold atoms and c is the light speed in vacuum. By fitting numerically the calculated curve (dotted line) from Eq. (1) to the measured MDSR signal (solid line), as shown in Fig. 1(c), we can determine the population distributions in the Zeeman sublevels $m=-1$, 0, $+1$ of the

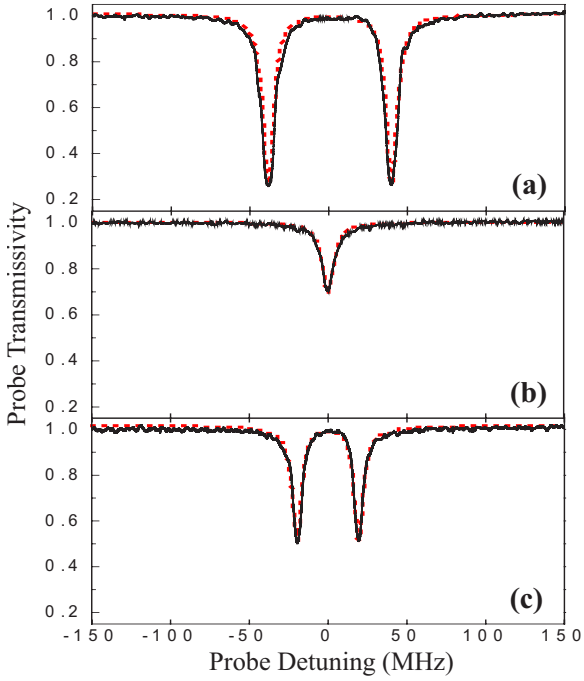

FIG. 3. (Color online) Transmission spectra of the probe beam for different pumping beam polarizations. Solid lines are the experimental results. Dotted lines are the theoretical fitting curves corresponding to (a) $P_{a_{-1}}=96\%$, $P_{a_0}=2\%$, and $P_{a_{+1}}=2\%$; (b) $P_{a_{-1}}=1\%$, $P_{a_0}=1\%$, and $P_{a_{+1}}=98\%$; and (c) $P_{a_{-1}}=1\%$, $P_{a_0}=98\%$, and $P_{a_{+1}}=1\%$. $N_{F1}=0.6\times10^{11}$ cm^{-3}. Other parameters are the same as in Fig. 1.

$5S_{1/2}$, F=1 level to be $P_{a_{-1}}=32\%$, $P_{a_0}=36\%$, $P_{a_{+1}}=32\%$.

To prepare atoms into a well-specified spin-polarized state, a polarized pumping beam E_b is added, which is on resonance with the transition from $5S_{1/2}$, F=1 to $5P_{1/2}$, F′=1 and propagates through the cold atoms with a small angle (about 2°) relative to the probe beam in the same plane [as shown in Figs. 2(a1) and 2(a2)]. The power of the pumping beam is set at 13.6 mW with a diameter of ~2 mm (which overlaps with the coupling and probe beams at the cold atomic cloud). The experimental procedure is the same as the one discussed above by switching on the coupling beam and this pumping beam at the same time as we turn off the MOT.

When the pumping beam is left-circularly polarized, as shown in Figs. 2(a1) and 2(b1) , all the ground-state populations in $5S_{1/2}$, F=1 are prepared in the $|a_{-1}\rangle$ state. In this case, when the weak, left-circularly polarized probe beam scans through the transition, only one simple EIT curve (related to the energy levels $|a_{-1}\rangle$, $|c_{-2}\rangle$, and $|b_{-2}\rangle$) is observed [Fig. 3(a)]. The two absorption peaks correspond to the dressed-state absorption due to the coupling field Ω_{c2}. The clean double-peak structure is a good indication that atoms are mostly prepared in the $|a_{-1}\rangle$ state. Similarly, when the pumping beam is right-circularly polarized, as shown in Figs. 2(a2) and 2(b2) , all the ground-state populations in $5S_{1/2}$, F=1 are prepared in the $|a_{+1}\rangle$ state. In this case, since no coupling occurs between states $|b_0\rangle$ and $|c_0\rangle$, no EIT system can be formed and only a single absorption peak is observed [Fig. 3(b)]. As the pumping beam is changed to be linearly polarized and propagates through cold atoms along the x direction, as shown in Figs. 2(a3) and 2(b3) , all the ground-state populations in $5S_{1/2}$, F=1 are prepared in the $|a_0\rangle$ state. Notice that the transition strength between states $5S_{1/2}$, F=1, m=0 and $5P_{1/2}$, F′=1, m′=0 is also zero [24]. In this case, the left-circularly polarized probe field Ω_{p1} and the coupling field Ω_{c1} (connecting states $|b_{-1}\rangle$ and $|c_{-1}\rangle$) form a single EIT system, as shown in Figs. 2(b3) and 3(c) . This EIT window is much narrower than the one for the left-circularly polarized pumping beam [Fig. 3(a)], since $\Omega_{c1}=\Omega_{c2}/2$. The clean single EIT curve again indicates the concentration of ground-state population in state $|a_0\rangle$, since any residual populations in other states will give rise to small peaks at other positions.

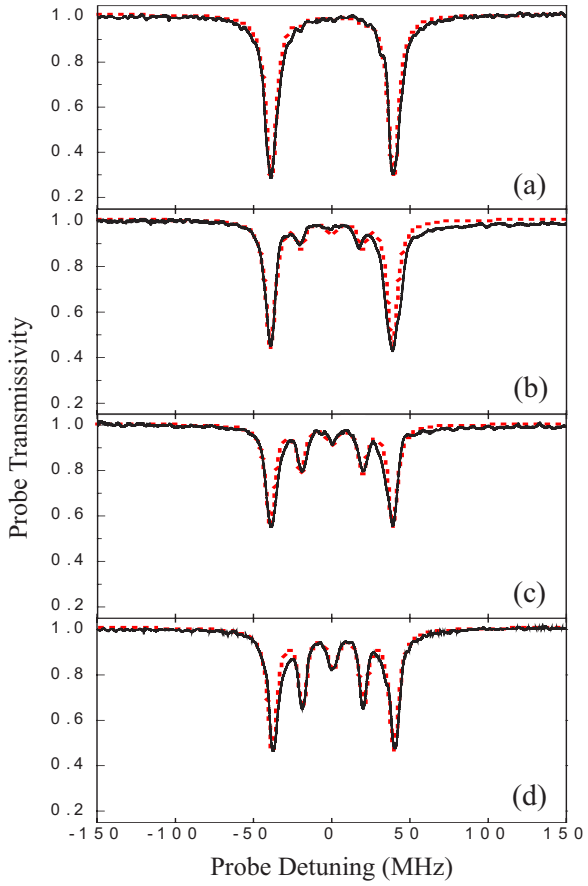

FIG. 4. (Color online) Transmission spectra of the probe beam for a left-circularly polarized pumping beam of different powers. Solid lines are the experimental results and dotted lines are the theoretical fitting curves.

Next, we theoretically calculated the probe beam susceptibilities using Eq. (1) and fit them to the experimentally measured results as given in Fig. 3. As one can see, excellent matches between the theoretical calculated results (dotted lines) and experimentally measured data (solid lines) are obtained, and the purities of the prepared spin-polarized states are quite high (>96%), not counting the atoms trapped in the $|b_0\rangle$ state. Note that the total density of atoms in the $5S_{1/2}$, F=1 states is $N_{F1}=1.2\times10^{11}$ cm^{-3} in the absence of the pumping beam, while N_{F1} becomes 0.6×10^{11} cm^{-3} in the presence of the polarized pumping beam with P_2 of about

13.6 mW. The total atomic population includes atomic populations in the Zeeman sublevels of $5S_{1/2}$, F=1 (N_{F1}) and $5S_{1/2}$, F=2(N_{F2}) states. Since the state $5S_{1/2}$, F=2, m=0 ($|b_0\rangle$) does not interact with any other states in the schemes [as shown in Figs. 1(c) and 2(b1)–2(b3)], a certain atomic population will be trapped in this $|b_0\rangle$ state as N_{F2}. The ratio between N_{F1} and N_{F2} changes as the polarized pumping beam is turned on, which modifies the total ground-state population on the $5S_{1/2}$, F=1 state (N_{F1}).

Using this technique, we cannot only prepare pure spin-polarized ground states in this multi-Zeeman-sublevel atomic system, but also create and determine any desired ground-state population distributions. By decreasing the power of the pumping beam P_2 in different pumping beam polarizations (as in the cases of Fig. 2), different ground-state population distributions can be obtained. Figure 4 shows different probe signals obtained at different powers of the left-circularly polarized pumping beam [Fig. 2(b1)] and the fitted results. When P_2=5 mW, a good fitting with the experimental data gives $P_{a_{-1}}$=92%, P_{a_0}=4%, and $P_{a_{+1}}$=4%, $N_{F1}=0.6\times10^{11}$ cm^{-3} as shown in Fig. 4(a). As the pumping power is increased to be larger than 5 mW, atoms will mostly be pumped into the $|a_{-1}\rangle$ state, as the case shown in Fig. 3(a). When P_2=1 mW, a ground-state population distribution of $P_{a_{-1}}$=64%, P_{a_0}=18%, $P_{a_{+1}}$=18%, as shown in Fig. 4(b), is obtained. As the pumping power is further reduced to 0.5 mW, the ground-state population distribution becomes $P_{a_{-1}}$=42%, P_{a_0}=33%, and $P_{a_{+1}}$=25% [Fig. 4(c)]. When P_2=50 μW, the ground-state population distribution is $P_{a_{-1}}$=33%, P_{a_0}=35%, and $P_{a_{+1}}$=32% [Fig. 4(d)], which is basically the same as the result when without the pumping beam [Fig. 1(c)]. Similarly, with right-circularly polarized or linearly polarized pumping beams at different powers, various other ground-state population distributions can be obtained. Actually, any desired ground-state population distributions can be realized by choosing appropriate pumping beam polarization and power, e.g., by entering the desired population distribution into the model, one can calculate the needed pumping beam power and polarization. This is a very powerful technique in preparing designed spin-polarized states in multi-Zeeman-sublevel atomic systems for using in quantum-state engineering.

In summary, we have developed an efficient and easy way to prepare desired spin-polarized ground-state population distributions in a multi-Zeeman-sublevel atomic system without using a strong magnetic field or microwave field and demonstrated a simple, all-optical scheme to determine the population distributions with high precision. We have shown that more than 96% state purity can be easily achieved in any one of the ground states, and any other desired state mixings can also be prepared and determined, which constitute complete spin-polarized quantum state engineering. Such prepared initial atomic states can be used for demonstrating quantum phase gates in four- and five-level atomic systems, improving quantum state storage in atomic assembles, preparing atomic states for entanglement, and many other quantum-information processing schemes.

We acknowledge funding supports by the National Natural Science Foundation of China (Grants No. 60325414, No. 60578059, and No. 10640420195) and 973 Program (Grant No. 2006CB921103).

[1] C. Liu *et al.*, Nature (London) **409**, 490 (2001).
[2] Q. A. Turchette *et al.*, Phys. Rev. Lett. **75**, 4710 (1995).
[3] C. Ottaviani, D. Vitali, M. Artoni, F. Cataliotti, and P. Tombesi, Phys. Rev. Lett. **90**, 197902 (2003); C. Ottaviani, S. Rebic, D. Vitali, and P. Tombesi, Phys. Rev. A **73**, 010301(R) (2006).
[4] X. B. Zou and W. Mathis, Phys. Rev. A **71**, 042334 (2005).
[5] Z.-B. Wang, K.-P. Marzlin, and B. C. Sanders, Phys. Rev. Lett. **97**, 063901 (2006).
[6] D. N. Matsukevich *et al.*, Phys. Rev. Lett. **96**, 030405 (2006).
[7] B. B. Blinov *et al.*, Nature (London) **428**, 153 (2004).
[8] S. E. Harris, Phys. Today **50**, 36 (1997).
[9] K. J. Boller, A. Imamoglu, and S. E. Harris, Phys. Rev. Lett. **66**, 2593 (1991).
[10] J. Gea-Banacloche, Y. Q. Li, S. Z. Jin, and M. Xiao, Phys. Rev. A **51**, 576 (1995).
[11] T. Chanelière *et al.*, Nature (London) **438**, 833 (2005).
[12] D. N. Matsukevich *et al.*, Phys. Rev. Lett. **96**, 033601 (2006).
[13] A. S. Parkins, P. Marte, P. Zoller, and H. J. Kimble, Phys. Rev. Lett. **71**, 3095 (1993).
[14] W. Dreves, H. Jansch, E. Koch, and D. Fick, Phys. Rev. Lett. **50**, 1759 (1983).
[15] P. Tremblay and C. Jacques, Phys. Rev. A **41**, 4989 (1990).
[16] B. Julsgaard *et al.*, J. Opt. B: Quantum Semiclassical Opt. **6**, 5 (2004).
[17] G. S. Summy *et al.*, J. Phys. B **30**, L541 (1997).
[18] G. Avila *et al.*, Phys. Rev. A **36**, 3719 (1987).
[19] B. P. Masterson, C. Tanner, H. Patrick, and C. E. Wieman, Phys. Rev. A **47**, 2139 (1993).
[20] N. D. Bhaskar, Phys. Rev. A **47**, R4559 (1993).
[21] L. S. Goldner *et al.*, Phys. Rev. Lett. **72**, 997 (1994).
[22] G. Klose, G. Smith, and P. S. Jessen, Phys. Rev. Lett. **86**, 4721 (2001).
[23] G. A. Smith, A. Silberfarb, I. H. Deutsch, and P. S. Jessen, Phys. Rev. Lett. **97**, 180403 (2006); J. Opt. B: Quantum Semiclassical Opt. **5**, 323 (2003).
[24] Bo Wang *et al.*, Opt. Lett. **31**, 3647 (2006).
[25] S. Li *et al.*, Phys. Rev. A **74**, 033821 (2006).